ACADEMIC PRESS

Available online at www.sciencedirect.com
SCIENCE DIRECT®

Journal of Catalysis 215 (2003) 208–219

JOURNAL OF CATALYSIS

www.elsevier.com/locate/jcat

Thiophene hydrodesulfurization over supported nickel phosphide catalysts

Stephanie J. Sawhill, Diana C. Phillips, and Mark E. Bussell *

Department of Chemistry, MS-9150, Western Washington University, Bellingham, WA 98225, USA

Received 9 August 2002; revised 23 December 2002; accepted 7 January 2003

Abstract

Silica-supported nickel phosphide (Ni_2P/SiO_2) catalysts have been prepared and characterized by X-ray diffraction (XRD), transmission electron microscopy (TEM), elemental analysis, X-ray photoelectron spectroscopy (XPS), and O_2 chemisorption measurements. Ni_2P/SiO_2 catalysts were synthesized from oxidic precursors by reduction in either flowing H_2 or a H_2S/H_2 mixture. XRD and TEM analysis of a 25 wt% Ni_2P/SiO_2 catalyst confirmed the presence of Ni_2P crystallites dispersed on the surface of the silica support. XPS analysis of a passivated 30 wt% Ni_2P/SiO_2 catalyst indicated the presence of two kinds of Ni species, as well as phosphide and phosphate species at the catalyst surface. Thiophene hydrodesulfurization (HDS) activities were measured for Ni_2P/SiO_2 catalysts with a wide range of Ni_2P loadings (5–35 wt%) and after different pretreatments. A 30 wt% Ni_2P/SiO_2 catalyst, when pretreated only by degassing in flowing He, was nearly 15 and 3.5 times more active than sulfided Mo/SiO_2 and Ni–Mo/SiO_2 catalysts, respectively, after 100 h on-stream. The HDS activities of the Ni_2P/SiO_2 catalysts correlated well with their O_2 chemisorption capacities, allowing calculation of a turnover frequency of 0.017 ± 0.002 s^{-1}. Based on XRD measurements of tested catalysts as well as catalysts subjected to H_2S/H_2 treatments at increasing temperatures, silica-supported Ni_2P shows excellent stability under HDS conditions.

Keywords: Nickel phosphide; Hydrotreating; Hydrodesulfurization; Thiophene

1. Introduction

Phosphorus is often used as an additive in commercial hydrotreating catalysts and, depending upon the method of phosphorus addition and the amount added, increases in hydrotreating activity can be achieved by including it in catalyst formulations [1–3]. Despite the fact that its effects on hydrotreating have been extensively studied, the role of added phosphorus is not well understood [2]. For catalysts supported on gamma-alumina (γ-Al_2O_3), the typical support for commercial hydrotreating catalysts, the possible effects for added phosphorus include increased mechanical and thermal stability of the alumina support due to the formation of $AlPO_4$, decreased interaction between molybdate species and the support which leads to the formation of MoS_2-like structures with altered particle morphologies, and increased catalyst acidity [1–3]. The influence of phosphorus has generally been observed to have a greater (and more positive) effect on hydrodenitrogenation (HDN) activity than on hydrodesulfurization (HDS) activity [2].

To more fully understand the role of phosphorus in hydrotreating catalysts as well as to explore the properties of a new class of materials—transition metal phosphides—a number of studies have recently appeared in the literature describing the HDN [4–13] and HDS [5,7,8,10–15] properties of bulk and supported metal phosphide catalysts. Focusing on HDS, silica-supported molybdenum phosphide (MoP/SiO_2) [10,14] and nickel phosphide (Ni_2P/SiO_2) [11, 13,15] catalysts have shown particular promise, with activities similar to or higher than those of sulfide-based catalysts. Given the need to develop highly active HDS catalysts to meet requirements for lower sulfur levels in fuels combined with the prospect of processing lower quality petroleum feedstocks, further investigation of phosphide-based hydrotreating catalysts is needed to evaluate their potential. Such research may also provide new insight into the role of phosphorus additives in hydrotreating catalysts, as the presence of small, highly dispersed metal (Co, Ni, Mo) phosphide particles in these catalysts under working conditions cannot be ruled out.

* Corresponding author.
E-mail address: mark.bussell@wwu.edu (M.E. Bussell).

0021-9517/03/$ – see front matter
doi:10.1016/S0021-9517(03)00018-6

In this study, we describe the preparation of Ni_2P/SiO_2 catalysts and their characterization via a variety of techniques and compare their HDS catalytic properties to those of sulfided Ni/SiO_2, Mo/SiO_2, and $Ni–Mo/SiO_2$ ($Ni/Mo = 0.5$) catalysts. Silica was chosen as the catalyst support in this study for two reasons. First, it is well known that phosphorus interacts strongly with γ-Al_2O_3, in many cases resulting in the formation of aluminum phosphates such as $AlPO_4$ at the surface of the support [2]. In this initial investigation of the catalytic properties of supported Ni_2P, therefore, it may have proven difficult to determine whether the observed properties are associated with changes of the support, modified interactions between Ni-containing phases and the support, or to Ni_2P itself. Second, the relatively inert nature of SiO_2 facilitated the development of a synthesis procedure for preparing supported Ni_2P, which we expect can be modified for other supports.

2. Experimental methods

2.1. Catalyst preparation

2.1.1. Ni_2P

Unsupported nickel phosphide (Ni_2P) was prepared following a procedure adapted from that described by Gopalakrishnan et al. [16]. An aqueous solution containing 3.67 g (12.6 mmol) $Ni(NO_3)_2 \cdot 6H_2O$ (Alfa Aesar, 99.9985%) and 17.5 g (132.5 mmol) of $(NH_4)_2HPO_4$ (Mallinckrodt, 99.9%) was stirred overnight and then heated to 360 K for approximately 48 h, yielding a greenish-yellow precipitate, which was collected by filtration and dried at 373 K. A portion of the solid ($NH_4NiPO_4 \cdot H_2O$) was subsequently reduced by heating from room temperature to 923 K at a rate of 1 K/min in flowing H_2 (150 mL/min), followed by cooling to room temperature in a continued flow of H_2. The unsupported Ni_2P was then flushed with He (60 mL/min) for 15 min and passivated in a 30 mL/min flow of a 1.0 mol% O_2/He mixture (Airgas) for 2 h. The He (Airgas, 99.999%) and H_2 (Airgas, 99.999%) were purified prior to use by passing through 5A molecular sieve (Alltech) and O_2 (Oxyclear) purification traps.

2.1.2. Ni_2P/SiO_2

Ni_2P/SiO_2 catalysts with theoretical Ni_2P loadings of 5, 10, 15, 20, 25, 30, and 35 wt% were prepared, with the details for the synthesis of a 20 wt% Ni_2P/SiO_2 catalyst given below. The silica (SiO_2) support (Cab-O-Sil, M-7D grade, 200 m^2/g) was calcined at 773 K for 3 h prior to use. Impregnating solutions were prepared by dissolving 4.901 g $Ni(NO_3)_2 \cdot 6H_2O$ (Alfa Aesar, 99.9985%) and 1.551 g $NH_4H_2PO_4$ (Baker, 99.1%) in approximately 10 mL water each. The nickel solution was added dropwise to 5.0 g of calcined silica until incipient wetness, followed by drying at 393 K, and calcination in air at 773 K for 3 h. The sample was then impregnated with the $NH_4H_2PO_4$ solution and dried at 393 K. The precursor, which had a Ni/P molar ratio of 2/1.6, was reduced in flowing hydrogen (150 mL/min) as the temperature was increased from room temperature to 923 K (1 K/min). The sample was then cooled to room temperature in the flowing H_2, flushed with flowing He (60 mL/min) for 15 min, and then passivated in a flow of 1.0 mol% O_2/He (30 mL/min) for 2 h to yield silica-supported Ni_2P. A similar procedure was used for the other Ni_2P loadings.

2.1.3. Sulfided Ni/SiO_2

A NiO/SiO_2 catalyst precursor was prepared with a Ni loading similar to that of the 30 wt% Ni_2P/SiO_2 catalyst. Calcined silica (5.0 g) was impregnated with a solution containing 8.402 g $Ni(NO_3)_2 \cdot 6H_2O$ to give the desired metal loading (30.1 wt% NiO). The resulting precursor was dried in a 393 K oven and calcined in air at 773 K for 3 h. The NiO/SiO_2 precursor was sulfided by heating from room temperature to 650 K (5.9 K/min) in a 60 mL/min flow of 3.0 mol% H_2S/H_2 and holding at 650 K for 2 h.

2.1.4. Sulfided Mo/SiO_2

A MoO_3/SiO_2 catalyst precursor (30.4 wt% MoO_3) was prepared as follows. Calcined silica (2.5 g) was impregnated with a solution of 1.374 g $(NH_4)_6Mo_7O_{24} \cdot 4H_2O$ to give the desired metal loading. The resulting precursor was dried in a 393 K oven and calcined in air at 773 K for 3 h. The MoO_3/SiO_2 precursor was sulfided as described above.

2.1.5. Sulfided $Ni–Mo/SiO_2$ ($Ni/Mo = 0.5$)

A $NiO–MoO_3/SiO_2$ catalyst precursor (7.9 wt% NiO, 30.4 wt% MoO_3) was prepared as follows. Calcined silica (5.0 g) was impregnated with a solution of 3.019 g $(NH_4)_6Mo_7O_{24} \cdot 4H_2O$ and dried at 393 K, then impregnated with a solution of 2.490 g $Ni(NO_3)_2 \cdot 6H_2O$ and dried at 393 K, and finally calcined in air at 773 K for 3 h. The $NiO–MoO_3/SiO_2$ precursor was sulfided as described above.

2.2. Catalyst characterization

2.2.1. X-ray diffraction measurements

X-ray diffraction (XRD) patterns were acquired on a Rigaku Geigerflex powder diffractometer using the Vaseline smear method. The diffractometer is outfitted with a Cu-K_α source ($\lambda = 1.5418$ Å) and is interfaced to a personal computer for data acquisition and analysis using Materials Data Incorporated (MDI) DataScan and Jade Plus 5.0 software. Catalyst samples, whether freshly prepared, tested in the HDS reactor, or subjected to a H_2S/H_2 pretreatment, were passivated in a flow of a 1 mol% O_2/He mixture as described above prior to mounting in the X-ray diffractometer. Catalyst precursors and Ni_2P/SiO_2 catalysts were pretreated as described above, except that the temperatures of the H_2S/H_2 treatment are those listed in Figs. 8 and 9.

2.2.2. Elemental analysis

Analysis of the composition of unsupported Ni_2P and of a 25 wt% Ni_2P/SiO_2 catalyst was carried out using inductively coupled plasma–atomic emission spectroscopy (ICP–AES).

2.2.3. Transmission electron microscopy measurements

TEM images were acquired using a JEOL 2010 high-resolution transmission electron microscope operating at 200 keV. Samples of the catalysts were placed on a 200 mesh copper grid coated with formvar and carbon.

2.2.4. XPS measurements

X-ray photoelectron spectroscopy (XPS) measurements were carried out using a Physical Electronics Quantum 2000 Scanning ESCA Microprobe system with a focused monochromatic Al-K_α X-ray (1486.7 eV) source and a spherical section analyzer. The XPS spectra were collected using a pass energy of 23.5 or 46.95 eV. The spectra were referenced to an energy scale with binding energies for $Cu(2p_{3/2})$ at 932.67 ± 0.05 eV and Au(4f) 84.0 ± 0.05 eV. Binding energies were corrected for sample charging using the C(1s) peak at 284.6 eV for adventitious carbon as a reference. Low-energy electrons and argon ions were used for specimen neutralization.

2.2.5. BET surface area and pulse chemisorption measurements

BET surface area measurements were obtained using a Micromeritics PulseChemisorb 2700 apparatus. Approximately 0.10 g of catalyst was placed in a quartz U-tube and degassed at room temperature in a 60 mL/min flow He for 30 min. This was followed by a 2-h degassing of the sample in a 45 mL/min flow He at 623 K and cooling to room temperature under flowing He. The BET measurements were carried out as described previously [17].

Oxygen (O_2)-pulsed chemisorption measurements were also carried out using the Micromeritics Pulse Chemisorb 2700 instrument. Chemisorption capacity measurements were conducted using a 10.3 mol% O_2/He mixture (Airco). Approximately 0.10 g of catalyst was degassed in 60 mL/min He at room temperature for 30 min and either reduced or sulfided prior to measurements. Reduced samples were pretreated by heating from room temperature to 673 K (6.3 K/min) in 60 mL/min H_2 and holding for 2 h. Sulfided samples were pretreated by heating from room temperature to 650 K (5.9 K/min) in a 60 mL/min flow of a 3.0 mol% H_2S/H_2 mixture and holding for 2 h. Sulfided samples were then reduced in a 60 mL/min flow H_2 at 623 K for 1 h. All samples were degassed in 45 mL/min He at 673 K for 1 h prior to measurements. The O_2 chemisorption capacity measurements were carried out at 196 K using a procedure published elsewhere [17].

2.3. Thiophene HDS activity measurements

Thiophene HDS activity measurements were carried out using an atmospheric pressure flow reactor, which has been described in detail elsewhere [17]. Activity measurements were carried out at a reaction temperature of 643 K using a reactor feed consisting of a 3.2 mol% thiophene/H_2 mixture.

Prior to the measurement of thiophene HDS activities, the Ni_2P/SiO_2 catalysts (or their oxidic precursors) were subjected to one of three different pretreatments (He degas only, H_2S/H_2, and H_2). All catalysts were subjected to a degas in He (60 mL/min) at room temperature for 30 min. For a H_2S/H_2 pretreatment, the degassed catalyst was sulfided by heating from room temperature to 650 K (5.9 K/min) in a 60 mL/min flow of 3.0 mol% H_2S/H_2 and holding at 650 K for 2 h. Samples of the oxidic precursor of a 20 wt% Ni_2P/SiO_2 catalyst were pretreated in the H_2S/H_2 mixture similarly, but at a temperature of either 650 or 823 K. The heating rate for the 823 K H_2S/H_2 pretreatment was 8.8 K/min. For a H_2 pretreatment, the degassed catalyst was reduced by heating from room temperature to 650 K (5.9 K/min) in 60 mL/min H_2 and holding at 650 K for 2 h. Following each pretreatment, the temperature was adjusted to the reaction temperature of 643 K and the flow was switched to the 3.2 mol% thiophene/H_2 reactor feed (50 mL/min). The reaction was carried out for over 100 h, with automated sampling of the gas effluent occurring at 1-h intervals. Thiophene HDS activities (nmol Th/(g_{cat} s)) were calculated from the total product peak areas calculated from the chromatogram after 100 h of reaction time.

3. Results

3.1. Catalyst characterization

Shown in Fig. 1 are XRD patterns for Ni_2P/SiO_2 catalysts with Ni_2P loadings in the range 10–30 wt%, as well as for unsupported Ni_2P and the SiO_2 support. The XRD pattern of the unsupported Ni_2P is similar to a reference pattern taken from the JCPDS powder diffraction file (Card 03-0953) [18], as well as XRD patterns for Ni_2P recently reported by others [9,11,19]. The elemental composition of the unsupported nickel phosphide was determined by ICP–AES to be $Ni_{1.93}P_{1.00}$.

The XRD patterns for the Ni_2P/SiO_2 catalysts show the same peaks as those observed for unsupported Ni_2P, with the peak intensity increasing with increasing Ni_2P loading, confirming that Ni_2P crystallites are present on the silica support. Using the Scherrer equation [20] and the full width at half maximum of the {111} reflection at 40.8°, a Ni_2P particle size of ~ 17.8 nm can be estimated for the 25 wt% Ni_2P/SiO_2 catalyst. An excess of phosphorus ($Ni/P = 2/1.6$) was necessary in the oxidic precursors of the Ni_2P/SiO_2 catalysts in order to obtain phase pure, silica-supported Ni_2P. These observations are consistent with those

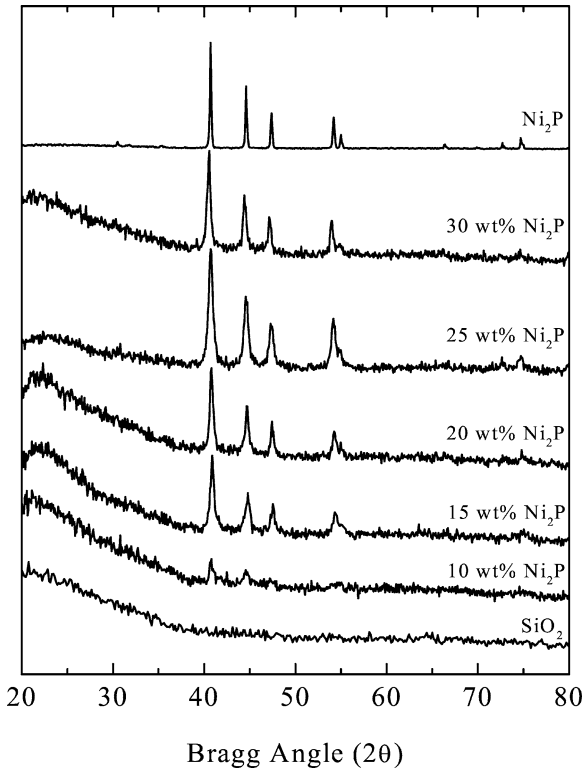

Fig. 1. X-ray diffraction patterns for the silica support, 10, 15, 20, 25, and 30 wt% Ni_2P/SiO_2 catalysts, and unsupported Ni_2P.

recently reported by others [11,19]. The elemental composition of the nickel phosphide phase of a 25 wt% Ni_2P/SiO_2 catalyst was determined to be $Ni_{1.8}P_{1.0}$ indicating that some excess P remained on the catalyst following reduction. Catalysts prepared with a Ni/P molar ratio of 2/1 contained substantial amounts of $Ni_{12}P_5$ (Card 22-1190 [18]) as determined by XRD. As will be discussed later, these catalysts deactivated rapidly under HDS conditions.

Shown in Fig. 2 are TEM images of a 25 wt% Ni_2P/SiO_2 catalyst. As indicated by Fig. 2a, the Ni_2P particle size ranges from approximately 5 to 30 nm. The high-resolution image in Fig. 2b shows a Ni_2P particle having a diameter of ~ 14 nm, the d-spacing value of 3.20 Å is assigned to the {001} crystallographic plane of Ni_2P, and is in agreement with the JCPDS powder diffraction file pattern for Ni_2P (Card 03-0953 [18]).

XPS spectra in the Ni(2p) and P(2p) regions for the Ni_2P precursor, unsupported Ni_2P, and a 30 wt% Ni_2P/SiO_2 catalyst are shown in Fig. 3. The XPS spectrum for the Ni_2P oxidic precursor shows Ni($2p_{3/2}$) and P($2p_{3/2}$) peaks at 856.2 and 133.0 eV, respectively. The P($2p_{3/2}$) binding energy is in good agreement with a value reported for P (133.3 eV) in $Ni_3(PO_4)_2$ [21] while the Ni($2p_{3/2}$) binding energy is in the range of those reported for Ni (855.6–856.6 eV) in $Ni(OH)_2$ [22]. As a result, the peaks at 856.2 and 133.0 eV are assigned to Ni^{2+} and P^{5+} species, respectively. Similar peaks are observed in the XPS spectra for unsupported Ni_2P and the 30 wt% Ni_2P/SiO_2 catalyst

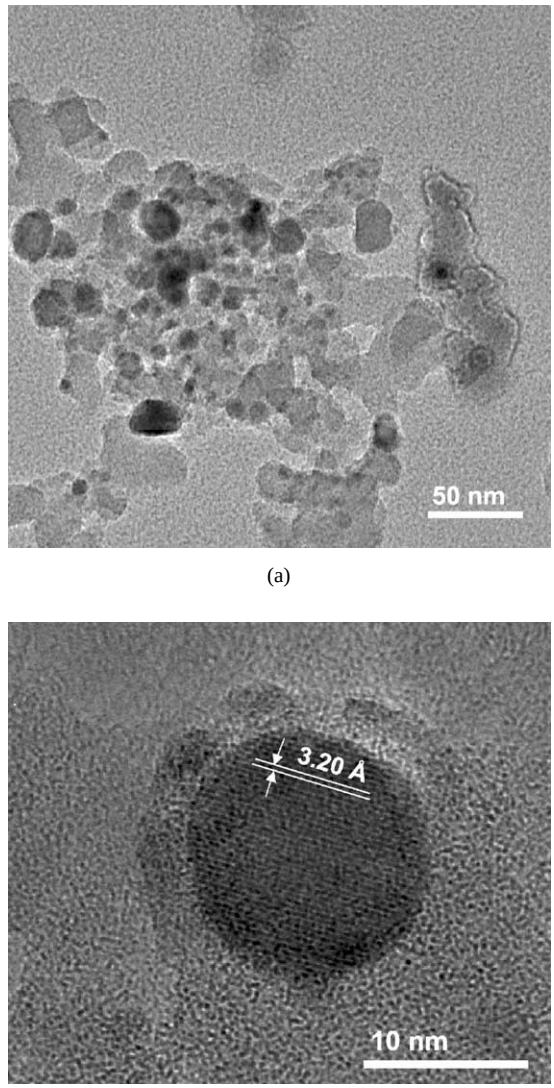

(a)

(b)

Fig. 2. TEM micrographs of a 25 wt% Ni_2P/SiO_2 catalyst.

and are assigned to Ni^{2+} and P^{5+} species in the oxide layer formed on the Ni_2P particles following TPR synthesis. For both the unsupported Ni_2P and the 30 wt% Ni_2P/SiO_2 catalyst, additional peaks are observed in the Ni($2p_{3/2}$) and P($2p_{3/2}$) regions at 853.1–853.5 and 129.4–129.5 eV, respectively, that are assigned to reduced Ni and P species in Ni_2P. These binding energies are consistent with those reported by Nemoshalenko et al. [23] for unsupported Ni_2P of 853.1 and 129.5 eV in the Ni($2p_{3/2}$) and P($2p_{3/2}$) regions, respectively. The Ni($2p_{3/2}$) binding energies are slightly higher than reported values for Ni metal (852.5–852.9 eV [24]) and lower than those reported for Ni in NiO (853.5–854.1 eV [24]), indicating that the Ni in Ni_2P bears a partial positive charge ($Ni^{\delta+}$). The P($2p_{3/2}$) binding energies are below the value reported for elemental phosphorus (130.2 eV [24]), consistent with the transfer of electron density from Ni to P in unsupported and silica-supported Ni_2P so that the phosphorus bears a partial negative charge

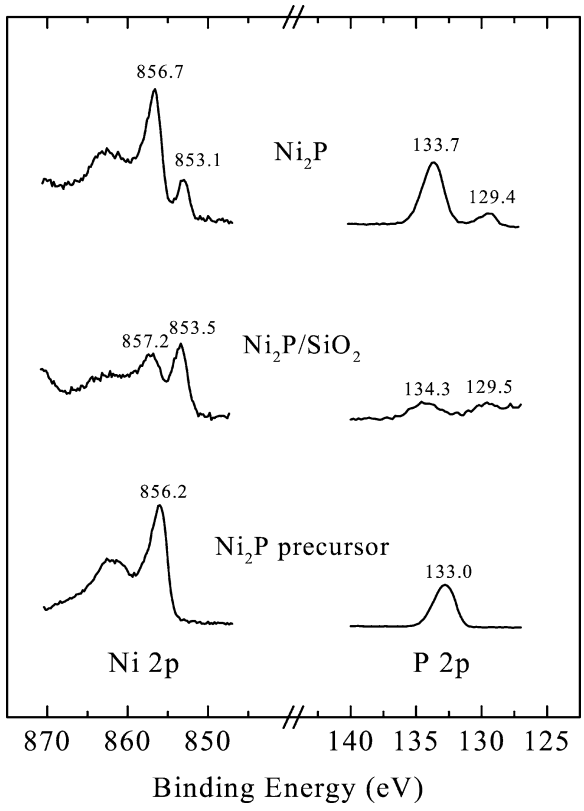

Fig. 3. XPS spectra in the Ni(2p) and P(2p) regions for an oxidic Ni_2P precursor, a 30 wt% Ni_2P/SiO_2 catalyst, and unsupported Ni_2P.

($P^{\delta-}$). Surface Ni and P concentrations were determined using XPS for 20 and 30 wt% Ni_2P/SiO_2 catalysts to be 69 atom% Ni and 31 atom% P, which are very similar to those expected from the bulk composition.

The BET surface areas and O_2 chemisorption capacities for the Ni_2P/SiO_2 and sulfided Ni/SiO_2, Mo/SiO_2, and Ni–Mo/SiO_2 catalysts are listed in Table 1. The O_2 chemisorption capacities of the Ni_2P/SiO_2 catalysts exhibit an increasing trend with Ni_2P loading up to 30 wt% and are generally higher than those of the sulfided Ni/SiO_2, Mo/SiO_2, and Ni–Mo/SiO_2 (Ni/Mo = 0.5) catalysts.

3.2. Catalyst evaluation and stability

Thiophene HDS activity data as a function of time on-stream for a 30 wt% Ni_2P/SiO_2 catalyst, as well as for sulfided Ni/SiO_2, Mo/SiO_2 and Ni–Mo/SiO_2 (Ni/Mo = 0.5) catalysts, are shown in Fig. 4. The Ni_2P/SiO_2 catalyst, which was pretreated only by degassing in flowing He, exhibited the highest HDS activity over the entire testing period. The HDS activities of the catalysts after 100 h on-stream are listed in Table 1 and are compared in Fig. 5. The 30 wt% Ni_2P/SiO_2 catalyst is 14.8 and 31.4 times more active than the sulfided Mo/SiO_2 and Ni/SiO_2 catalysts, respectively, and is 3.5 times more active than the sulfided Ni–Mo/SiO_2 catalyst (Ni/Mo = 0.5). Thiophene HDS activities were measured for Ni_2P/SiO_2 catalysts with other Ni_2P loadings in the range 5–35 wt% and these activities are listed in Table 1 and are plotted as a function of the O_2 chemisorption capacities of the catalysts in Fig. 6. The HDS activities of the Ni_2P/SiO_2 catalysts increase with Ni_2P loading with a maximum activity achieved for a loading of 30 wt%, exhibiting a trend that mirrors that of the chemisorption capacities. The low chemisorption capacity for the 35 wt% Ni_2P/SiO_2 catalyst is the average of two similar values measured for two different catalysts. At this time, it is unclear why this catalyst does not fit the trend observed for the lower loading catalysts. As shown in Fig. 6, the HDS activities of the catalysts (with loadings up to 30 wt%) correlate well

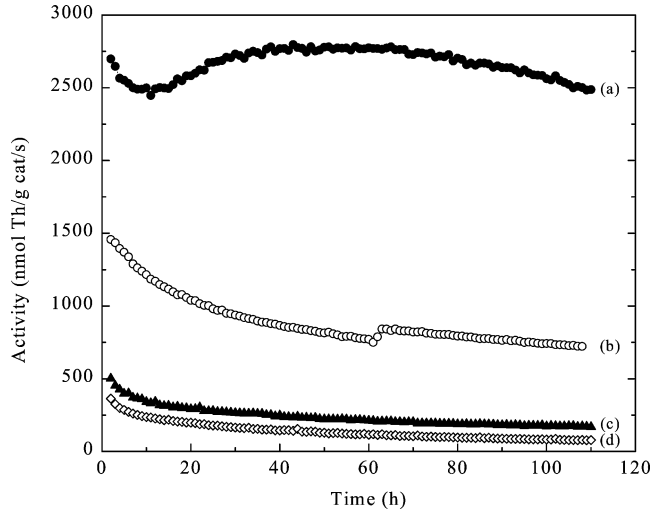

Fig. 4. Thiophene HDS activity data for (a) 30 wt% Ni_2P/SiO_2, (b) sulfided Ni–Mo/SiO_2 (Ni/Mo = 0.5), (c) sulfided Mo/SiO_2, and (d) sulfided Ni/SiO_2 catalysts.

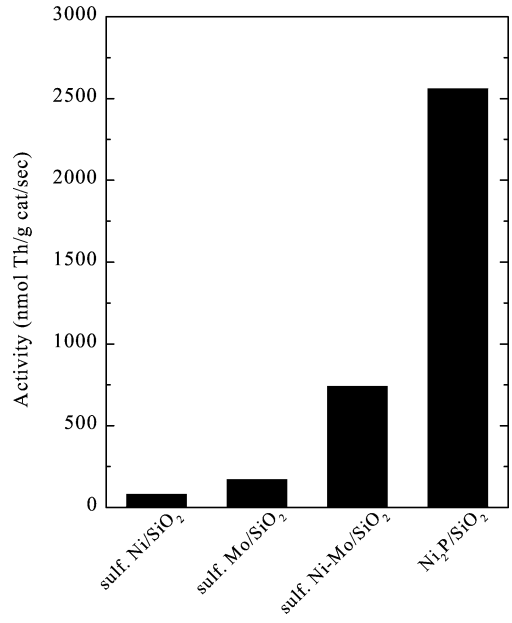

Fig. 5. Comparison of the HDS activities after 100 h on-stream for 30 wt% Ni_2P/SiO_2, sulfided Ni/SiO_2, Mo/SiO_2, and Ni–Mo/SiO_2 (Ni/Mo = 0.5) catalysts.

Table 1
Data for Ni_2P/SiO_2 and sulfide catalysts

Catalyst	BET surface area (m^2/g)	Chemisorption capacity ($\mu mol\ O_2/g$)	HDS activity (nmol Th/(g_{cat} s))
5 wt% Ni_2P/SiO_2	102.5	29.9	544.5
10 wt% Ni_2P/SiO_2	96.2	67.2	1156.0
15 wt% Ni_2P/SiO_2	93.5	91.4	2031.4
20 wt% Ni_2P/SiO_2	103.1	123.9	2284.5
25 wt% Ni_2P/SiO_2	80.6	153.5	2458.0
30 wt% Ni_2P/SiO_2	66.1	166.1	2562.1
35 wt% Ni_2P/SiO_2	64.2	78.9	2551.1
Sulf. Ni/SiO_2	112.6	71.9	81.5
Sulf. Mo/SiO_2	91.5	18.1	173.2
Sulf. Ni–Mo/SiO_2	96.4	22.8	741.7
Sulf. 20 wt% Ni_2P/SiO_2[a]	78.7	72.0	2002.3

[a] Catalyst prepared by H_2S/H_2 treatment of the oxidic precursor at 823 K.

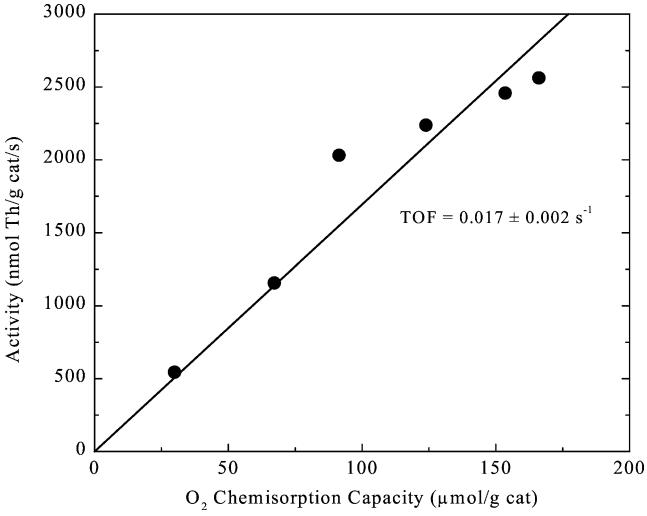

Fig. 6. Correlation of thiophene HDS activity with O_2 chemisorption capacity for Ni_2P/SiO_2 catalysts.

with their O_2 chemisorption capacities. From the slope of the linear regression plot, a turnover frequency (TOF) of $0.017 \pm 0.002\ s^{-1}$ can be calculated if it is assumed one O_2 molecule adsorbs to each active site. As mentioned earlier, Ni_2P/SiO_2 catalysts prepared from oxidic precursors with a molar ratio $Ni/P = 2/1$ yielded catalysts containing a significant $Ni_{12}P_5$ impurity. The HDS activity of the Ni_2P/SiO_2 catalysts containing $Ni_{12}P_5$ impurities deactivated rapidly after being brought on stream. A 20 wt% Ni_2P/SiO_2 catalyst containing a significant $Ni_{12}P_5$ impurity (as determined by XRD) had an activity of 720.7 nmol Th/g cat/s after 100 h on-stream, just 32.2% of the HDS activity of a phase pure 20 wt% Ni_2P/SiO_2 catalyst.

To determine the stability of Ni_2P/SiO_2 catalysts under HDS reaction conditions, X-ray diffraction patterns were acquired for fresh and tested 20 wt% Ni_2P/SiO_2 catalysts that are shown in Fig. 7. After 110 h on-stream in the HDS reactor, no significant changes are observed in the

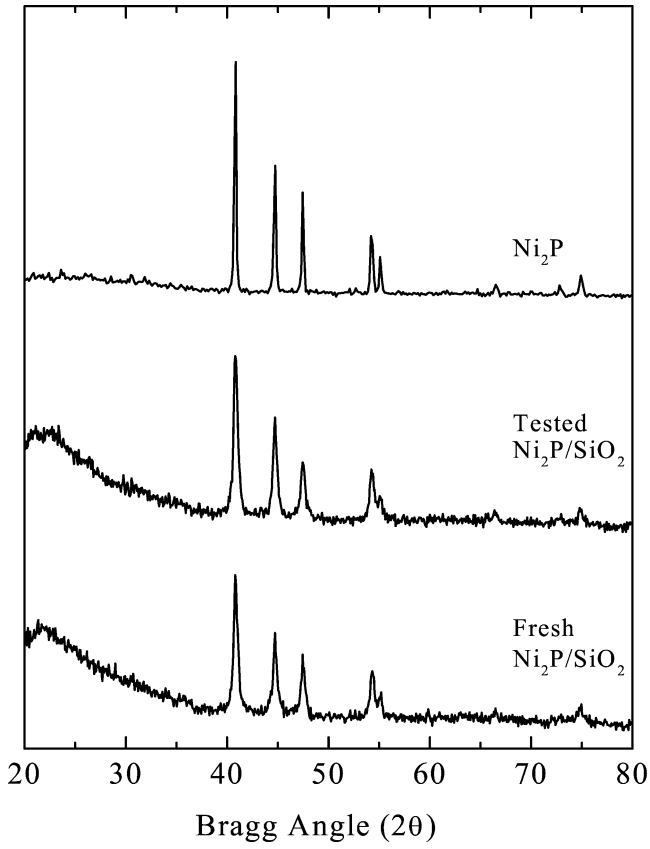

Fig. 7. X-ray diffraction patterns for fresh and tested (110 h on-stream) 20 wt% Ni_2P/SiO_2 catalysts, as well as for unsupported Ni_2P.

XRD pattern of the tested 20 wt% Ni_2P/SiO_2 catalyst when compared to the fresh catalyst, indicating no change in the bulk structure of the supported Ni_2P particles. The only apparent change in the XRD patterns is a slight increase in intensity of the Ni_2P reflections for the tested catalyst. Using the Scherrer equation, a Ni_2P particle size of 19.6 nm is calculated for the tested 25 wt% Ni_2P/SiO_2 catalyst, which is larger than the value for the fresh catalyst of 17.8 nm. To further access the stability of the silica-supported Ni_2P under reaction conditions, samples of a 20 wt% Ni_2P/SiO_2 catalyst were sulfided at temperatures in the range 623–1023 K and then analyzed by XRD. Other than small increases in the intensity of the Ni_2P reflections following H_2S/H_2 pretreatment (see Fig. 8), there is no evidence for the formation of new crystalline phases in the 20 wt% Ni_2P/SiO_2 catalyst despite being subjected to H_2S/H_2 treatment at temperatures as high as 1023 K.

3.3. Effect of pretreatment on catalyst activity

Thiophene HDS activity measurements were carried out for samples of a 20 wt% Ni_2P/SiO_2 catalyst following degas-only, reduction, and H_2S/H_2 pretreatments, as well as for the oxidic precursor to this catalyst following degas-only and H_2S/H_2 pretreatments (at 650 and 823 K). The latter set of activity measurements was motivated by the observation

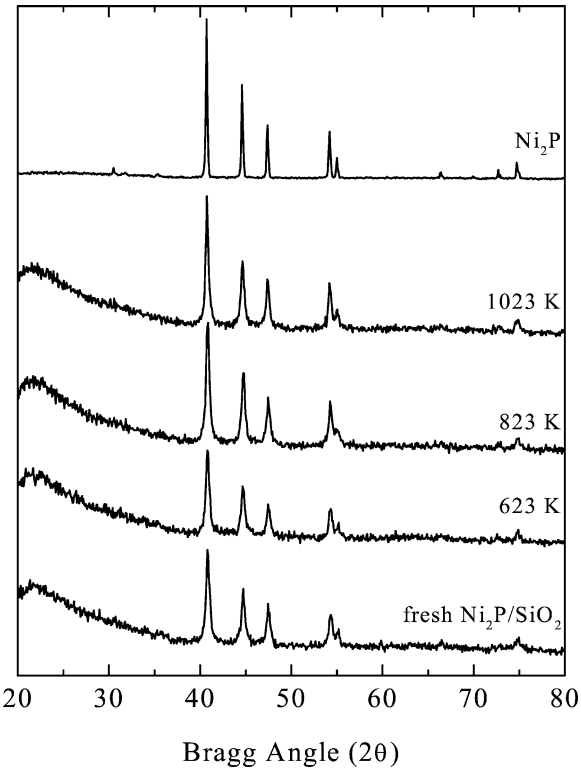

Fig. 8. X-ray diffraction patterns for 20 wt% Ni_2P/SiO_2 catalysts subjected to H_2S/H_2 pretreatments at the indicated temperatures.

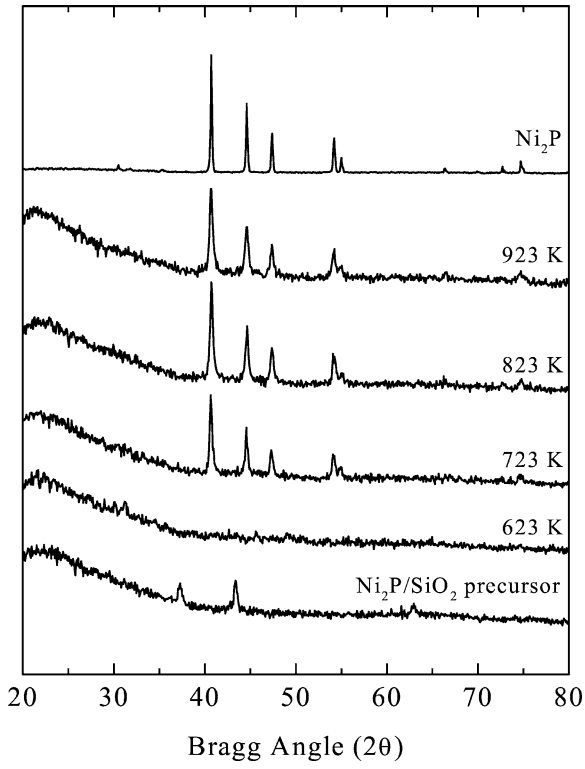

Fig. 9. X-ray diffraction patterns for the oxidic precursor of the 20 wt% Ni_2P/SiO_2 catalyst, subjected to H_2S/H_2 pretreatments at the indicated temperatures.

that the oxidic precursor of the 20 wt% Ni_2P/SiO_2 catalyst could be reduced to the phosphide catalyst using a pretreatment in a 3.0 mol% H_2S/H_2 mixture at a temperature of 723 K or higher (see Fig. 9). As shown at the bottom of the figure, the oxidic precursor of the 20 wt% Ni_2P/SiO_2 catalyst shows XRD peaks consistent with the presence of crystalline NiO (Card 06-0595 [18]) on the silica support. Upon pretreatment in flowing H_2S/H_2 at increasing temperatures, the XRD peaks of NiO disappear (623 K) and XRD peaks for Ni_2P appear (723 K) and grow stronger (823 K).

The data plotted in Fig. 10 show interesting trends in the effect of pretreatment on HDS activity. For the Ni_2P/SiO_2 catalysts, there is a small but significant effect of pretreatment on HDS activity with the reduced and sulfided catalysts 4.0 and 12.8% more active, respectively, after 100 h than the catalyst pretreated only by degassing in He (see Fig. 11). Independent of the pretreatment, the Ni_2P/SiO_2 catalysts all show the same trend with the HDS activity increasing over the first 24–48 h and then decreasing slightly over the remaining time on-stream. In all cases, the 20 wt% Ni_2P/SiO_2 catalysts were more active or of equal activity at the end of the testing period compared to when they were initially brought on-stream, further indicating that they have excellent stability under HDS conditions.

The oxidic precursor of the 20 wt% Ni_2P/SiO_2 catalyst, when pretreated by He degas-only or H_2S/H_2 at 650 K, exhibits a strongly increasing HDS activity over time indicating that the surfaces of the catalysts are evolving into more

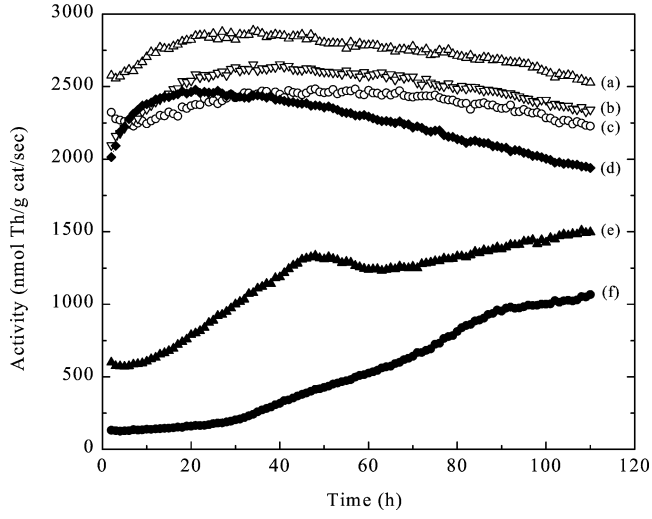

Fig. 10. Thiophene HDS activity data for 20 wt% Ni_2P/SiO_2 catalysts subjected to (a) H_2S/H_2, (b) reduction, and (c) degas-only pretreatments, as well as for the oxidic precursor subjected to H_2S/H_2 pretreatments at (d) 823 K, (e) 650 K, or (f) a degas-only pretreatment.

active forms. If the oxidic precursor is sulfided at 823 K, which reduces the Ni phase to Ni_2P as described earlier, its initial HDS activity is almost as high as those of the 20 wt% Ni_2P/SiO_2 catalysts subjected to the different pretreatments. The HDS activity of the oxidic precursor sulfided at 823 K increases over the first 20 h, but then decreases somewhat more rapidly over the remaining time on-stream

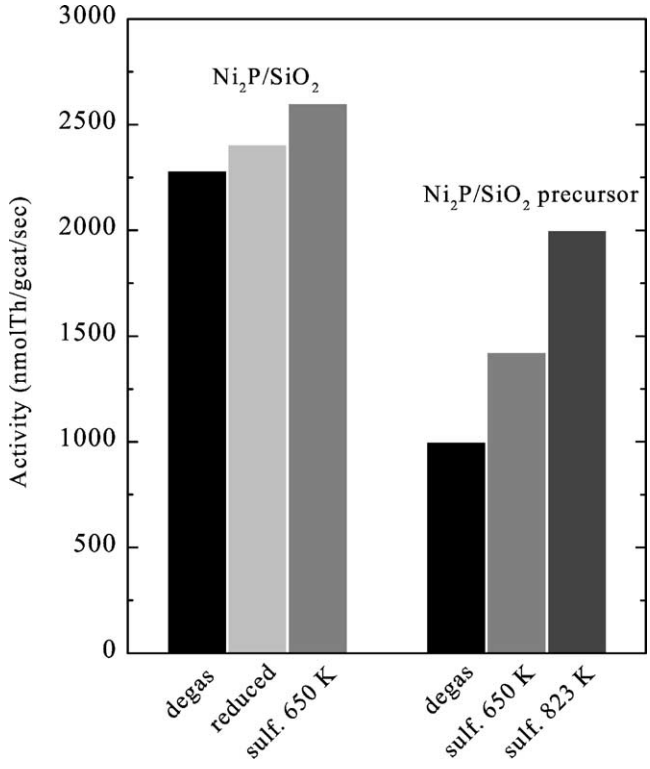

Fig. 11. Comparison of the HDS activities after 100 h on-stream for 20 wt% Ni_2P/SiO_2 catalysts subjected to degas-only, H_2S/H_2 and H_2 pretreatments, and for the oxidic precursor to this catalyst subjected to degas-only and H_2S/H_2 pretreatments.

when compared to the 20 wt% Ni_2P/SiO_2 catalysts prepared by H_2 TPR. A Ni_2P particle size of 26.9 nm was calculated for the oxidic precursor sulfided at 823 K and then tested in the HDS reactor, which compares well with the particle size of 27.7 nm calculated for the freshly sulfided precursor.

4. Discussion

It has been known for many years that the catalytic properties of transition metals can be substantially modified by combining them with main group elements. In some cases, it has been possible to carry out systematic investigations in which catalytic activities have been measured for compounds of a transition metal with different main group elements for a particular reaction. For example, molybdenum carbide (β-Mo_2C), nitride (γ-Mo_2N), and phosphide (MoP) are more active for thiophene HDS than is sulfided Mo when these materials are dispersed on an oxide support [14,17,25]. Such studies may ultimately lead to the development of new catalysts for industrial processes.

As indicated by the activity results shown in Figs. 4 and 5, Ni is a poor HDS catalyst when in a sulfided form (i.e., sulfided Ni/SiO_2). This observation is consistent with results reported by others for sulfided Ni catalysts in both unsupported [26,27] and supported [28–31] form, although Prins and co-workers observed sulfided Ni to have a higher activity than sulfided Mo when both materials were supported on carbon [32]. The beneficial HDS catalytic properties typically associated with Ni come from its use as a promoter of Mo- and W-based catalysts [1,3]. As with Mo, however, the catalytic properties of Ni can be substantially altered by combining it with different main group elements, in this case P. The results presented in this study, which are consistent with those recently published by Oyama and co-workers [11,13,15], indicate that silica-supported Ni_2P has high activity for HDS. Ni_2P/SiO_2 catalysts are substantially more active for thiophene HDS than are sulfided Ni/SiO_2, Mo/SiO_2, and $Ni–Mo/SiO_2$ ($Ni/Mo = 0.5$) catalysts.

The synthesis procedure described here for silica-supported Ni_2P catalysts differs somewhat from those recently reported by others [11,15,19]. Oyama and co-workers [11,15] utilized a single impregnation of a silica support with a solution of $Ni(NO_3)_2 \cdot 6H_2O$ and $NH_4H_2PO_4$ having a molar ratio of $Ni/P = 1/2$ or $2/2$, adding several drops of nitric acid to the impregnating solutions to keep nickel phosphates from precipitating. Following drying, the catalyst precursor was calcined and then reduced via TPR in flowing H_2 to a maximum temperature of 850 K. Stinner et al. [19] carried out a sequential impregnation of a silica support with $Ni(NO_3)_2 \cdot 6H_2O$ and $NH_4H_2PO_4$ with drying steps after each impregnation to give a precursor with $Ni/P = 2/1.3$. Following calcination, the oxidic precursor was reduced to silica-supported Ni_2P by TPR in a flowing 5 mol% H_2/N_2 mixture to a maximum temperature of 1023 K.

The synthesis described in the current study involved sequential impregnation of silica with Ni and P containing solutions (to give a molar ratio of $Ni/P = 2/1.6$) with calcination only after the Ni impregnation. The oxidic precursors were reduced to give Ni_2P/SiO_2 catalysts via TPR in flowing H_2 to a maximum temperature of 923 K. The Ni/P molar ratio and maximum TPR temperature employed were intermediary to those used by the other researchers. Attempts to prepare Ni_2P/SiO_2 catalysts using oxidic precursors prepared with a stoichiometric molar ratio of $Ni/P = 2/1$ yielded P deficient catalysts as indicated by the presence of $Ni_{12}P_5$. Stinner et al. [19] examined the effects of the Ni/P molar ratio and maximum TPR temperature, as well as the flow rate and composition of the reducing gas (H_2 or 5 mol% H_2/N_2), on the synthesis of silica-supported nickel phosphides. Pure silica-supported Ni_2P could not be prepared for molar ratios $Ni/P > 2/1.3$, and the optimal synthesis utilized the diluted reducing gas (5 mol% H_2/N_2), high flow rates (200–600 mL/min) and a maximum TPR temperature of 1023 K. The authors concluded that these conditions minimized the partial pressure of H_2O in the catalyst pores, and facilitated the formation and diffusion of volatile P-containing species into Ni particles on the support. The results reported here as well as those of Oyama and co-workers [11, 15] indicate that pure silica-supported Ni_2P can be pre-

pared using pure H_2 as the reducing gas, and that the maximum TPR temperature can be lowered to 850–923 K if a greater excess of P is used in the oxidic precursor ($Ni/P \leqslant 2/1.6$).

The oxidic precursors prepared by Oyama and co-workers [11,15] and Stinner et al. [19] were calcined following addition of $Ni(NO_3)_2 \cdot 6H_2O$ and $NH_4H_2PO_4$ to the silica support. Depending upon the Ni/P molar ratio, calcination would be expected to produce nickel phosphates, or a mixture of NiO and nickel phosphates on the silica. In contrast, the synthesis described in the current study utilized calcination only after impregnation of silica with $Ni(NO_3)_2 \cdot 6H_2O$, which should yield supported NiO. Following subsequent impregnation with $NH_4H_2PO_4$, the oxidic precursor is simply dried, which would be expected to give adsorbed phosphate species on the NiO/SiO_2 precursor. Despite the apparent separation of the Ni and P species in the oxidic precursor, TPR in flowing H_2 yielded phase pure Ni_2P on the silica support as confirmed by XRD and TEM. Interestingly, this synthesis procedure appears to give Ni_2P/SiO_2 catalysts with a higher dispersion of Ni_2P than is achieved by methods involving calcination after impregnation of the support with both $Ni(NO_3)_2 \cdot 6H_2O$ and $NH_4H_2PO_4$. A 25 wt% Ni_2P/SiO_2 catalyst was found to have an average crystallite size of 17.8 nm and an O_2 chemisorption capacity of 140.3 μmol/g. This crystallite size is smaller than the values reported by Wang et al. [11] and Stinner et al. [19] of 20 and 45 nm, respectively, for Ni_2P/SiO_2 catalysts with Ni_2P loadings less than 10 wt%.

Elemental analysis of a 25 wt% Ni_2P/SiO_2 catalyst gave a bulk composition of $Ni_{1.8}P_{1.0}$ for the supported Ni_2P particles while XPS measurements yielded an average surface composition of $Ni_{2.2}P_{1.0}$ for 20 and 30 wt% Ni_2P/SiO_2 catalysts. The elemental analysis indicates that the P content of the silica-supported Ni_2P is slightly greater than the amount expected for Ni_2P that is not surprising given the excess of P used in the catalyst synthesis, while the surface of the catalysts have the expected stoichiometry within the error bar of the XPS measurements. Wang et al. [11] measured a higher surface P content for their Ni_2P/SiO_2 catalyst, $Ni_{1.0}P_{1.0}$ but some P was lost during catalytic testing as the spent catalyst had a surface composition of $Ni_{1.3}P_{1.0}$. Based upon ^{31}P NMR measurements, Stinner et al. [19] concluded that no silicon phosphates formed at the surface of Ni_2P/SiO_2 catalysts prepared by TPR of oxidic precursors in flowing H_2. NMR signals associated with phosphate species ($H_nPO_4^{(3-n)-}$, $P_2O_4^{4-}$, and $(PO_3^-)_n$) were detected, presumably in the form of adsorbed species on the support. Using gravimetric measurements, Oyama et al. [33] observed that the excess P used in the impregnation is present in the oxidic precursor as a surface phosphate (most likely P_2O_5), but that most of this is lost as PH_3 during TPR. These researchers found that some residual P, possibly in the form of P_2O_5 on the silica support, does remain on the Ni_2P/SiO_2 catalysts after TPR.

The XPS spectra for unsupported Ni_2P and a 30 wt% Ni_2P/SiO_2 catalyst (see Fig. 3) show peaks for oxidized Ni and P species found in the surface passivation layer on the Ni_2P particles and, probably, due to P-containing species on the support, but also show peaks at 853.1–831.5 and 129.4–129.5 eV that are assigned to Ni and P species, respectively, in Ni_2P. These binding energies indicate a slight transfer of electron density from Ni to P, which is consistent with the interpretation by others of XPS spectra for amorphous Ni–P alloys [34,35]. As discussed by Stinner et al. [19], the short Ni–Ni metal distance in Ni_2P indicates strong metal bonding and this material does exhibit metallic character. At this time, it is unclear how the metallic properties of Ni_2P relate to the high HDS activity of Ni_2P/SiO_2 catalysts.

As indicated by the HDS activities compared in Fig. 4, a 30 wt% Ni_2P/SiO_2 catalyst is dramatically more active than sulfided Mo/SiO_2 and Ni/SiO_2 catalysts, as well as 3.5 times more active than a sulfided Ni–Mo/SiO_2 catalyst ($Ni/Mo = 0.5$). The Ni_2P/SiO_2 catalyst is also twice as active (after 100 h on-stream) as a 25 wt% MoP/SiO_2 catalyst tested under the identical HDS reaction conditions [14]. It should be noted that commercial hydrotreating catalysts most often are supported on γ-Al_2O_3, in part because a higher dispersion of the active sulfide phases can be achieved. In this study, silica was used as the support for the sulfide catalysts so that an additional variable was not introduced in the comparison between the Ni_2P/SiO_2 and sulfide catalysts. It should be noted, however, that the dispersion of the sulfided Mo/SiO_2 and Ni–Mo/SiO_2 catalysts is not high and could be improved by using alumina as the support. Using more industrially relevant hydrotreating conditions and alumina as the support for the comparison sulfide catalyst, Oyama et al. [15] recently reported a Ni_2P/SiO_2 catalyst to be more active than a commercial sulfided Co–Mo/Al_2O_3 catalyst (Ketjenfine 756). Importantly, the Ni_2P/SiO_2 catalyst achieved high HDS activity with the difficult to desulfurize compounds, 4-methyldibenzothiophene and 4,6-dimethyldibenzothiophene.

To gain further insight into the HDS properties of Ni_2P/SiO_2 catalysts, activity measurements were carried out for catalysts with Ni_2P loadings in the range 5–35 wt%. A maximum in HDS activity was observed for the 30 wt% Ni_2P/SiO_2 catalyst, which also had the highest O_2 chemisorption capacity. The HDS activities of the Ni_2P/SiO_2 catalysts correlated well with their O_2 chemisorption capacities (see Fig. 6) except for the 35 wt% Ni_2P/SiO_2 catalyst. From the slope of the linear regression analysis of the data, a TOF of $0.017 \pm 0.002\ s^{-1}$ was calculated. This value can be compared to a TOF of $0.013 \pm 0.001\ s^{-1}$ measured for sulfided Mo/Al_2O_3 catalysts (1.5–20 wt%) at 693 K [25]. In addition to the higher reaction temperature (693 vs 643 K), the TOF for the sulfided Mo/Al_2O_3 catalysts was calculated based upon the HDS activities of the catalysts after 24 h on-stream, instead of after 100 h as was the case for the Ni_2P/SiO_2 catalysts. Together, these factors suggest that the TOF de-

termined for the sulfided Mo/Al_2O_3 catalysts with a wide range of Mo loadings would be somewhat lower under the conditions used in the current study, and perhaps similar to the TOF of 0.0096 s^{-1} calculated for the sulfided Mo/SiO_2 catalyst (30.4 wt% MoO_3) tested in the current study. We conclude that the HDS activity of the Ni_2P/SiO_2 catalysts can be traced to both a high site density and a high TOF. The high chemisorption capacities of the Ni_2P/SiO_2 catalysts are not surprising as it is expected that Ni_2P can adsorb O_2 on all surface planes and the correlation shown in Fig. 6 indicates that O_2 is a good probe of active site densities.

An explanation for the high TOF of the Ni_2P/SiO_2 catalysts is currently lacking. The TOF of 0.017 ± 0.002 s^{-1} is dramatically higher than that calculated for the sulfided Ni/SiO_2 catalyst (30.1 wt% NiO) of 0.0011 s^1. Clearly, the sites on the silica-supported Ni_2P provide the needed structural and electronic characteristics for the efficient cleavage of the C–S bonds of thiophene as well as the hydrogenation of the resulting adsorbed hydrocarbon and sulfur species to give gas phase products. There were no significant differences between the thiophene HDS product distribution for a 20 wt% Ni_2P/SiO_2 catalyst and those reported previously for MoP/SiO_2 and sulfided Mo/SiO_2 catalysts [14], suggesting that the mechanisms of the reaction are similar over the different catalysts. Characterization of the adsorption sites at the surface of Ni_2P/SiO_2 catalysts will be necessary in order to more fully understand the high thiophene HDS activity of these catalysts.

Under the conditions of thiophene HDS at atmospheric pressure, Ni_2P/SiO_2 catalysts exhibit excellent stability as reflected in their resistance to deactivation. The chemical stability of these catalysts under sulfiding conditions of either a 3.2 mol% thiophene/H_2 feed (at 650 K) or a 3.0 mol% H_2S/H_2 gas mixture (at 623–1023 K), as determined by XRD, is consistent with this conclusion. Wang et al. [11] used XRD to analyze a spent Ni_2P/SiO_2 catalyst after testing on-stream in a mixed feed containing dibenzothiophene, quinoline, benzofuran, and tetralin at 643 K and observed the Ni_2P reflections to remain, but noted the growth of a new peak that they tentatively assigned to Ni_7P_3. This observation indicates the loss of some P from the silica-supported Ni_2P and is consistent with XPS measurements that showed a decrease in the P/Ni ratio at the surface from 1.00 to 0.77. While the XRD results of Wang et al. [11] differ slightly from ours, it should be noted that they observed an almost identical trend in HDS activity as that reported here (see Figs. 4 and 10) in that the dibenzothiophene HDS activity of the Ni_2P/SiO_2 catalyst increased over approximately the first 20 h and then decreased slightly for the remainder of the time on-stream. A possible explanation of the slight deactivation of the Ni_2P/SiO_2 catalysts may be the sintering of the nickel phosphide particles under HDS conditions. Based upon XRD patterns for fresh and tested 20 wt% Ni_2P/SiO_2 catalysts (see Fig. 7), an increase in average crystallite size from 17.8 to 19.6 nm was calculated. This growth of Ni_2P crystallites under reaction conditions may result in a slight decrease in the site density and a concomitant decrease in HDS activity.

The HDS activity of the Ni_2P/SiO_2 catalysts exhibited a mild sensitivity to the pretreatment employed, with a 20 wt% Ni_2P/SiO_2 catalyst pretreated in a flowing H_2S/H_2 mixture at 650 K being 8.5 and 12.8% more active than samples of the same catalyst pretreated in either H_2 or He, respectively (see Fig. 11). While XRD indicates no change occurs in the bulk structure of supported Ni_2P particles following H_2S/H_2 pretreatment at temperatures in the range 623–1023 K (see Fig. 8), we do not yet have conclusive results on how pretreatment in a flowing H_2S/H_2 mixture affects the surface of the supported Ni_2P particles. It is possible that some sulfur is incorporated into the surface of the Ni_2P particles during H_2S/H_2 pretreatment leading to formation of a surface phosphosulfide layer that is more active than pure Ni_2P. Based on recently published EXAFS measurements of spent Ni_2P/SiO_2 catalysts, Oyama and coworkers [13] concluded that some sulfur is incorporated into silica-supported Ni_2P during the HDS of dibenzothiophene and that the active catalytic phase is a surface phosphosulfide layer. The EXAFS spectra of the spent Ni_2P/SiO_2 catalysts were not consistent with a reference spectrum of $NiPS_3$, a phase which Robinson et al. [4] observed to convert to Ni_2P when pretreated in flowing H_2S/H_2. It is not yet possible, therefore, to propose a composition for a surface phosphosulfide layer at the surface of the silica-supported Ni_2P particles. It may be that the formation of a surface phosphosulfide layer under reaction conditions is responsible for the increase in HDS activity observed in the first 24–48 h after the Ni_2P/SiO_2 catalysts are brought on-stream (see Figs. 4 and 10).

While the synthesis presented here for the preparation of Ni_2P/SiO_2 catalysts, as well as those described recently by others [11,15,19], utilizes TPR in flowing H_2 to produce the silica-supported phosphide phase, it is also possible to prepare Ni_2P/SiO_2 catalysts from their oxidic precursors by a H_2S/H_2 pretreatment. As shown in Fig. 9, H_2S/H_2 pretreatment of an oxidic precursor of a 20 wt% Ni_2P/SiO_2 catalyst at temperatures in the range 723–1023 K gives silica-supported Ni_2P with no evidence of any crystalline impurities. Using XRD, Robinson and van Gestel [4] observed nickel orthophosphate ($Ni_3(PO_4)_2$) to convert to Ni_2P by a pretreatment of the orthophosphate salt in a 10 vol% H_2S/H_2 mixture at 643 K, but to our knowledge this approach has not been reported for the synthesis of oxide-supported Ni_2P catalysts.

The oxidic precursor to a 20 wt% Ni_2P/SiO_2 catalyst that was pretreated only by degassing in He initially had a very low HDS activity, but which increased monotonically over the course of 110 h on-stream (see Fig. 10). When coupled with the observation that Ni_2P/SiO_2 catalysts can be prepared by H_2S/H_2 pretreatment of their oxidic precursors, this observation suggests that the reducing conditions present in the HDS reactor at the reaction temperature of

643 K may slowly transform the oxidic precursors to silica-supported Ni_2P. If samples of this same precursor were subjected to H_2S/H_2 pretreatments at 650 or 823 K, the initial HDS activities of the catalysts were higher, and continued to increase either over the testing period (650 K pretreatment) or over the first 20 h (823 K pretreatment). These observations are consistent with the conclusion that the H_2S/H_2 pretreatment converts the oxidic precursor to silica-supported Ni_2P, thereby increasing the initial HDS activity of the catalysts. Unexpected, however, is the observation that the oxidic precursor sulfided at 823 K displays a somewhat different trend in HDS activity than the Ni_2P/SiO_2 catalysts prepared by TPR in flowing H_2. The HDS activity of the oxidic precursor sulfided at 823 K peaks earlier and then falls more rapidly than those of the catalysts prepared by H_2 TPR. After 100 h on-stream, this catalyst has an activity that is 8.5–22% lower than the 20 wt% Ni_2P/SiO_2 catalysts prepared by H_2 TPR and subsequently subjected to the different pretreatments (see Fig. 11). Possible explanations for the lower HDS activity of the 20 wt% Ni_2P/SiO_2 catalyst prepared via this method is that the reduction in H_2S/H_2 resulted in a poorer dispersion of the Ni_2P on the support, or that sulfur becomes incorporated at the surface of the Ni_2P particles thereby blocking sites. The 20 wt% Ni_2P/SiO_2 catalyst prepared via H_2S/H_2 treatment of the oxidic precursor had an average crystallite size of 27.7 nm and an O_2 chemisorption capacity of 72.0 μmol/g, which can be compared with values of 22.3 nm and 123.9 μmol/g for the 20 wt% Ni_2P/SiO_2 catalyst prepared via H_2 TPR. It should be noted that no attempt was made to optimize the Ni_2P/SiO_2 catalyst synthesis in which the oxidic precursors were reduced in the sulfiding mixture. Further investigation will be necessary to determine whether this procedure for converting oxidic precursors to Ni_2P/SiO_2 catalysts is a viable method for preparing high HDS activity catalysts.

5. Conclusions

Ni_2P/SiO_2 catalysts have been prepared by two methods in which oxidic precursors were reduced via TPR in either flowing H_2 or a H_2S/H_2 mixture. Synthesis of phase pure Ni_2P on the silica support was accomplished only when an excess of P ($Ni/P = 2/1.6$) was incorporated into the supported precursor. XPS analysis of unsupported Ni_2P and Ni_2P/SiO_2 catalysts indicates a slight transfer of electron density from Ni to P. The Ni_2P/SiO_2 catalysts have high thiophene HDS activity compared to sulfide-based catalysts, with a 30 wt% Ni_2P/SiO_2 catalyst being nearly 3.5 times more active than a sulfided Ni–Mo/SiO_2 catalyst ($Ni/Mo = 0.5$). In addition, the Ni_2P/SiO_2 catalysts exhibit excellent stability under HDS conditions and show promise for use in commercial hydrotreating catalysts.

Acknowledgments

This research was supported by the National Science Foundation under Grant CHE-0101690. A portion (TEM, ICP-AES, XPS) of the research described in this paper was performed in the Environmental Molecular Sciences Laboratory (EMSL), a national scientific user facility sponsored by the Department of Energy's Office of Biological and Environmental Research and located at Pacific Northwest National Laboratory. The authors acknowledge EMSL staff members: Mark Engelhard, Todd Hart, Chongmin Wang, and Chuck Peden for their assistance in data acquisition and interpretation, and for helpful discussions. The authors also thank Professor S. Ted Oyama for providing copies of accepted manuscripts prior to publication.

References

[1] H. Topsøe, B. Clausen, F.E. Massoth, in: J.R. Anderson, M. Boudart (Eds.), Catalysis: Science and Technology, Vol. 11, Springer, Berlin, 1996, p. 1.
[2] R. Iwamoto, J. Grimblot, Adv. Catal. 44 (1999) 417.
[3] T. Kabe, A. Ishihara, W. Qian, Hydrodesulfurization and Hydrodenitrogenation: Chemistry and Engineering, Wiley–VCH, Weinheim, 1999.
[4] W.R.A.M. Robinson, J.N.M. van Gestel, J. Catal. 161 (1996) 539.
[5] W. Li, B. Dhandapani, S.T. Oyama, Chem. Lett. (1998) 207.
[6] C. Stinner, R. Prins, T. Weber, J. Catal. 191 (2000) 1.
[7] S.T. Oyama, P. Clark, V.L.S. Teixiera da Silva, E.J. Lede, F.G. Requejo, J. Phys. Chem. B 105 (2001) 4961.
[8] P. Clark, W. Li, S.T. Oyama, J. Catal. 200 (2001) 140.
[9] C. Stinner, R. Prins, T. Weber, J. Catal. 203 (2001) 187.
[10] P. Clark, X. Wang, S.T. Oyama, J. Catal. 207 (2002) 256.
[11] X. Wang, P. Clark, S.T. Oyama, J. Catal. 208 (2002) 321.
[12] S.T. Oyama, P. Clark, X. Wang, T. Shido, Y. Iwasawa, S. Hayashi, J.M. Ramallo-Lopez, F.G. Requejo, J. Phys. Chem. B 106 (2002) 1913.
[13] S.T. Oyama, X. Wang, Y.-K. Lee, K. Bando, F.G. Requejo, J. Catal. 210 (2002) 207.
[14] D.C. Phillips, S.J. Sawhill, R. Self, M.E. Bussell, J. Catal. 207 (2002) 266.
[15] S.T. Oyama, X. Wang, F.G. Requejo, T. Sato, Y. Yoshimura, J. Catal. 209 (2002) 1.
[16] J. Gopalakrishnan, S. Pandey, K.K. Rangan, Chem. Mater. 9 (1997) 2113.
[17] P.A. Aegerter, W.W.C. Quigley, G.J. Simpson, D.D. Ziegler, J.W. Logan, K.R. McCrea, S. Glazier, M.E. Bussell, J. Catal. 164 (1996) 109.
[18] JCPDS Powder Diffraction File, International Centre for Diffraction Data, Swarthmore, PA, 2000.
[19] C. Stinner, Z. Tang, M. Haouas, T. Weber, R. Prins, J. Catal. 208 (2002) 456.
[20] C. Suryanarayana, M.G. Norton, X-Ray Diffraction: A Practical Approach, Plenum Press, New York, 1998.
[21] R. Franke, T. Chasse, P. Streubel, A. Meisel, J. Electron Spectrosc. Relat. Phenom. 56 (1991) 381.
[22] P. Dufresne, E. Payen, J. Grimblot, J.P. Bonnelle, J. Phys. Chem. 85 (1981) 2344.
[23] V.V. Nemoshalenko, V.V. Didyk, V.P. Krivitskii, A.I. Senekevich, Russ. J. Inorg. Chem. 28 (1983) 2182. [English translation.]
[24] D. Briggs, M.P. Seah (Eds.), Practical Surface Analysis by Auger and X-Ray Photoelectron Spectroscopy, Wiley, New York, 1983.

[25] K.R. McCrea, J.W. Logan, T.L. Tarbuck, J.L. Heiser, M.E. Bussell, J. Catal. 171 (1997) 255.
[26] T.A. Pecoraro, R.R. Chianelli, J. Catal. 67 (1981) 430.
[27] S. Harris, R.R. Chianelli, J. Catal. 86 (1984) 400.
[28] M.J. Ledoux, O. Michaux, G. Agostini, J. Catal. 102 (1986) 275.
[29] P.J. Mangnus, A. Riezebos, A.D. van Langeveld, J.A. Moulijn, J. Catal. 151 (1995) 178.
[30] J. Frimmel, M. Zdrazil, J. Catal. 167 (1997) 286.
[31] J. Quartararo, S. Mignard, S. Kasztelan, J. Catal. 192 (2000) 307.
[32] J.C. Duchet, E.M. van Oers, V.H.J. de Beer, R. Prins, J. Catal. 80 (1983) 386.
[33] S.T. Oyama, X. Wang, Y.-K. Lee, W.J. Chun, K. Asakura, submitted for publication.
[34] Z. Hu, J. Shen, Y. Chen, M. Lu, Y. Hsia, J. Non-Cryst. Solids 159 (1993) 88.
[35] M.G. Thube, S.K. Kulkarni, D. Huerta, A.S. Nigavekar, Phys. Rev. B 34 (1986) 6874.